

Probing the Top-Yukawa Coupling in Associated Higgs production with a Single Top Quark

Chih-Ting Lu 盧致廷 (NTHU)

National Tsing Hua University, Hsinchu, Taiwan

CEPC physics and computing workshop

◆ Collaborators for this work :

- Prof. Kingman Cheung

- Prof. Jae Sik Lee

- Dr. Jung Chang

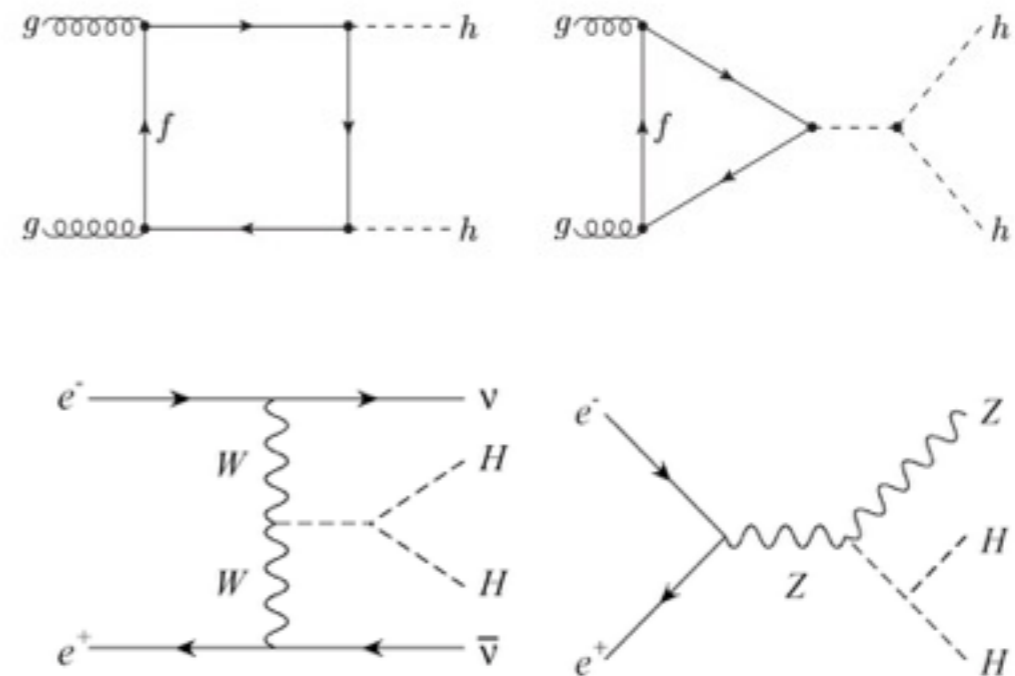
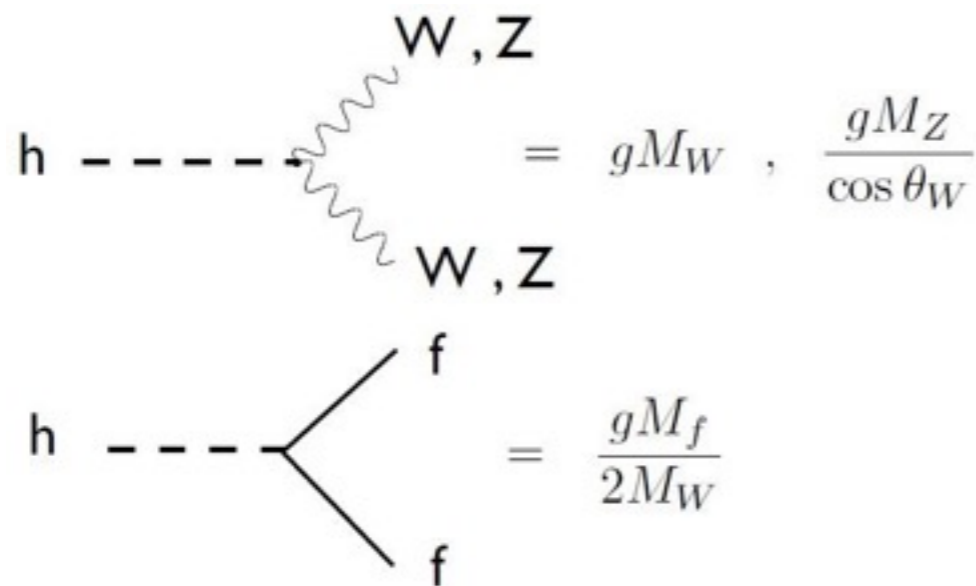
- Ref : **arXiv:1403.2053** **JHEP 1405 (2014) 062**

Outline

- 1. Motivation
- 2. Highlight some experimental results for the Higgs boson at the LHC
- 3. Formalism and Results from Higgs Precision (Higgcision) analysis
- 4. Probing the Top-Yukawa Coupling in Associated Higgs production with a Single Top Quark at the LHC
- 5. Discussion

Motivation

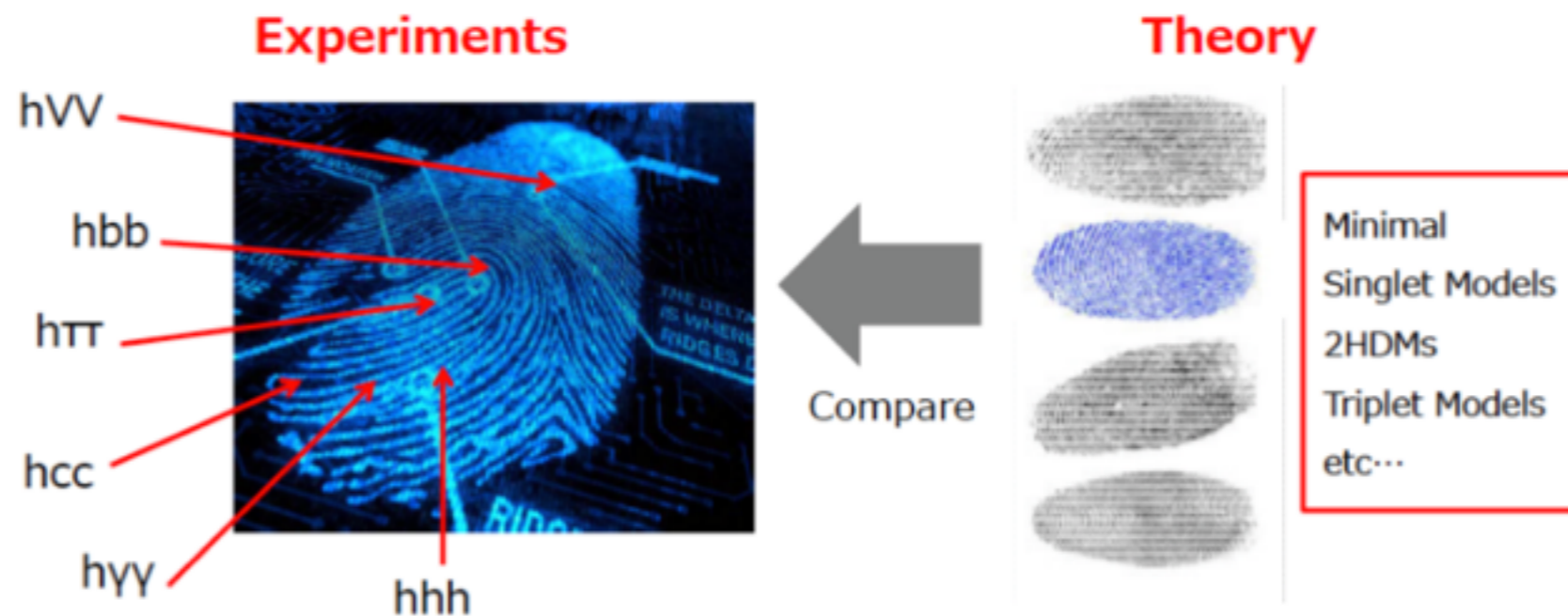
- Why is it important for the discovery of the Higgs boson ?
- 1. It is a byproduct of the BEH mechanism, so if we discover the Higgs boson, then we can confirm the BEH mechanism ! (It is NOT just a new scalar particle !)
- 2. New type of interactions :



Motivation

Shinya KANEMURA
U. of TOYAMA

All SM parameters are found
Precision = Energy frontier



Fingerprinting new physics models

Motivation

R. Santos
ISEL & CFTC (U. Lisboa)


Status of the CP-conserving 2HDM

Alignment and wrong-sign Yukawa

The **Alignment (SM-like) limit** - all tree-level couplings to fermions and gauge bosons are the SM ones.

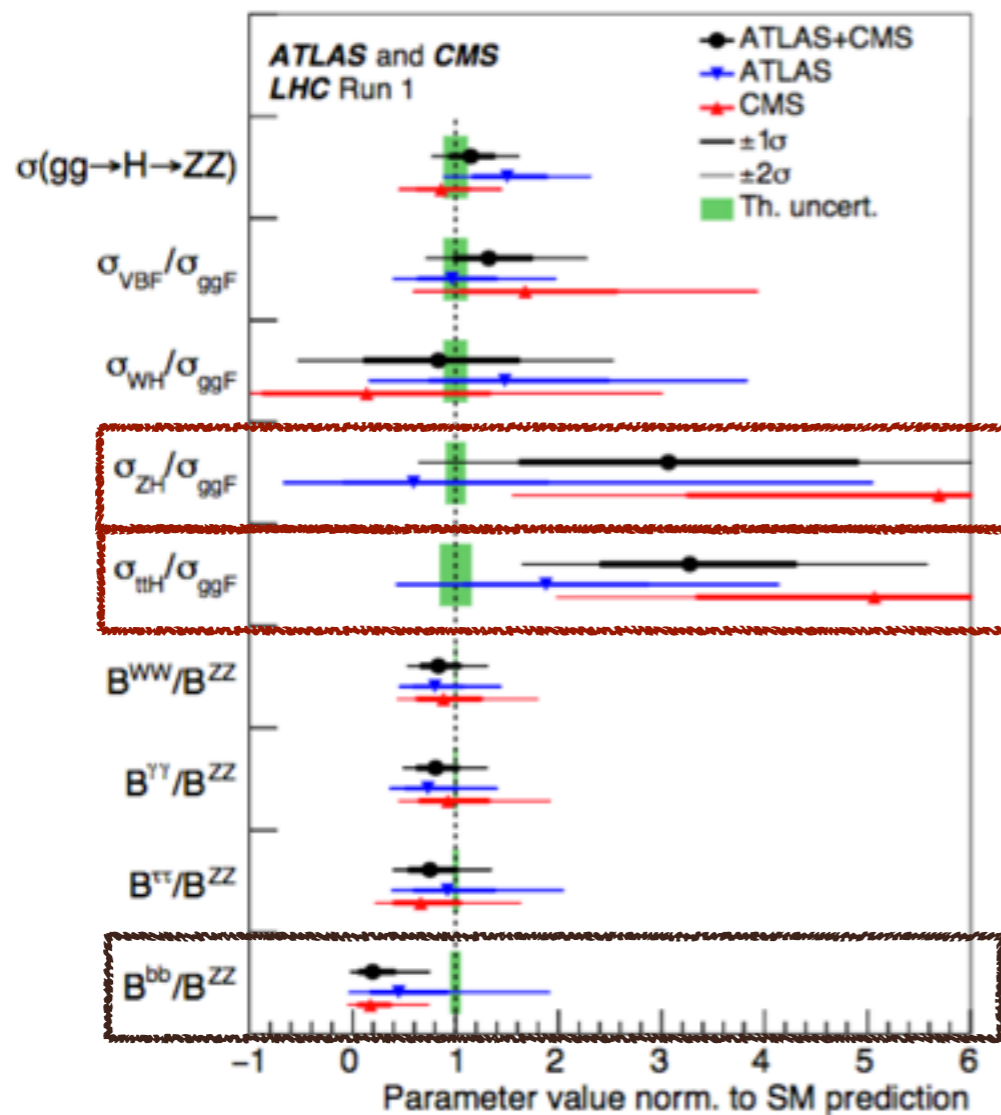
$$\sin(b-a) = 1 \quad \Leftrightarrow \quad k_D = 1; \quad k_U = 1; \quad k_W = 1$$

Wrong-sign Yukawa coupling - at least one of the couplings of h to down-type and up-type fermion pairs is opposite in sign to the corresponding coupling of h to VV (in contrast with SM).

$$k_D k_W < 0 \quad \text{or} \quad k_U k_W < 0$$


The actual sign of each κ_i depends on the chosen range for the angles.

Highlight some experimental results for the Higgs boson at the LHC



arXiv:1606.02266

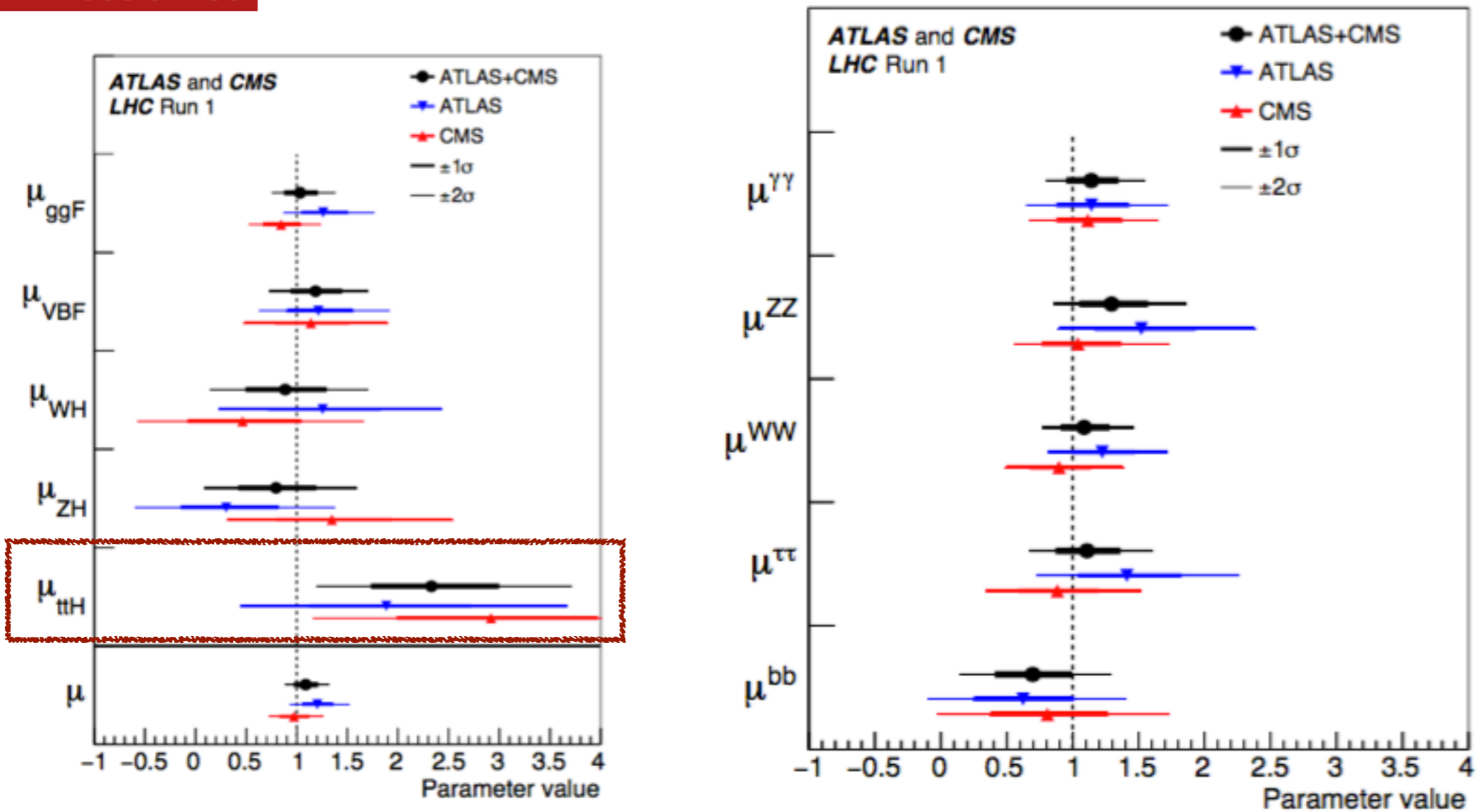
$$\frac{\sigma_{ZH}/\sigma_{ggF}}{\text{the same ratio in SM}} = 3.2 \pm 1.4$$

$$\frac{\sigma_{ttH}/\sigma_{ggF}}{\text{the same ratio in SM}} = 3.3 \pm 0.9$$

$$\frac{B^{bb}/B^{ZZ}}{\text{the same ratio in SM}} = 0.19 \pm 0.21$$

Highlight some experimental results for the Higgs boson at the LHC

arXiv:1606.02266



Highlight some experimental results for the Higgs boson at the LHC

- CMS search for the Associated Higgs production with a Single Top Quark

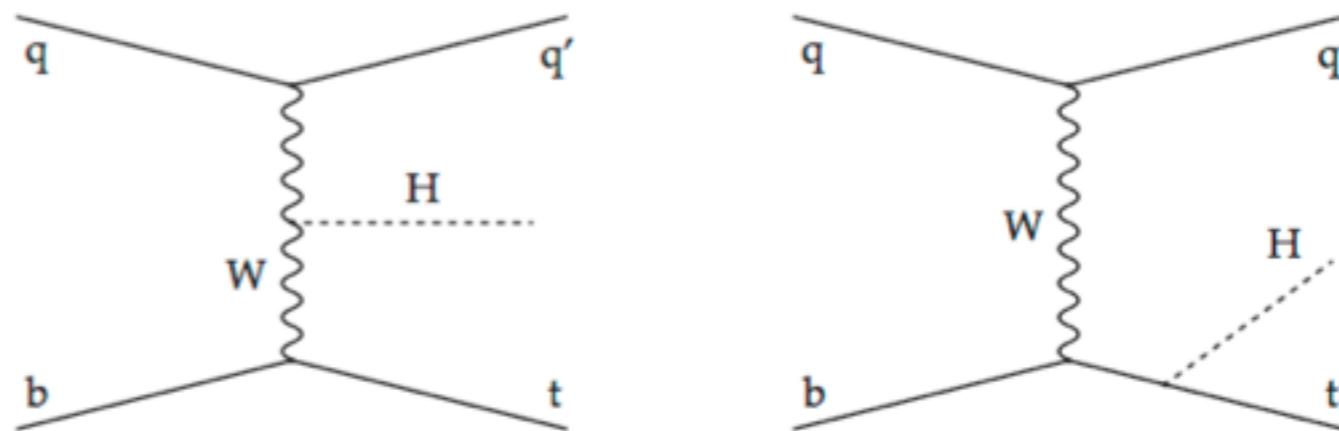


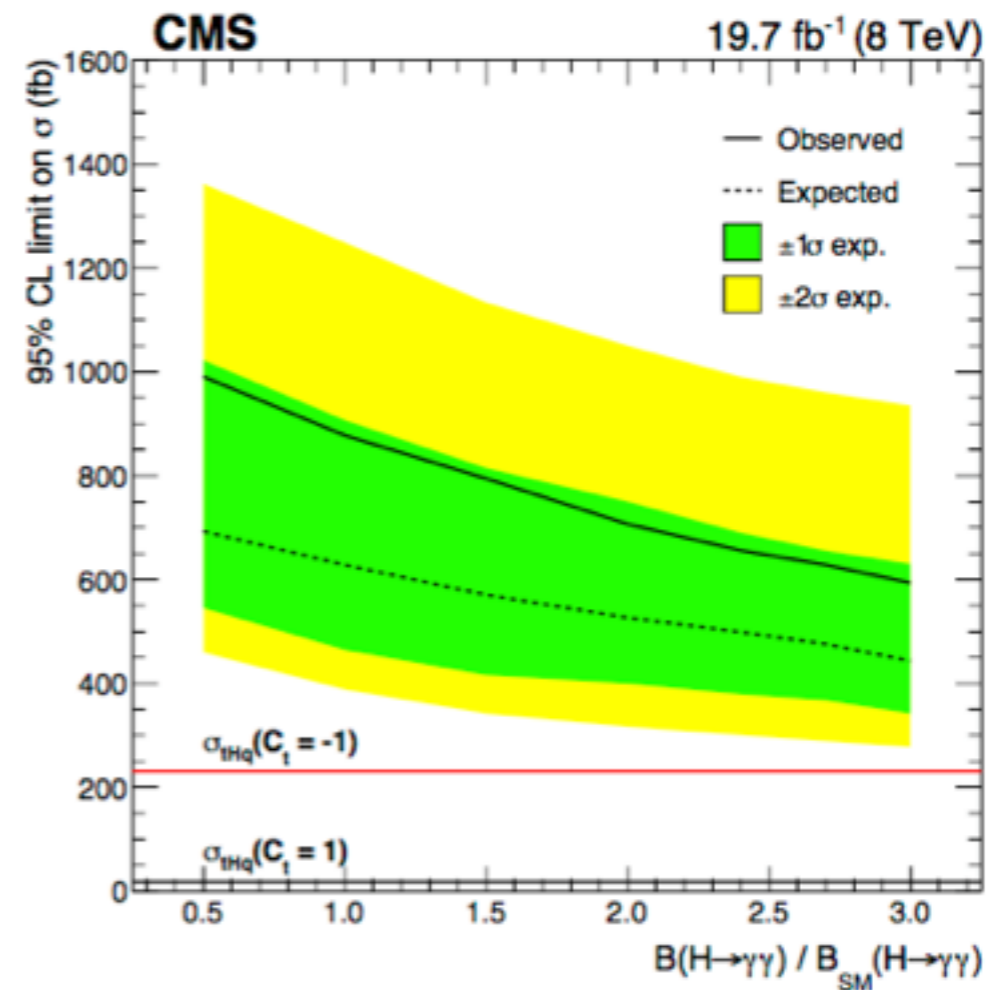
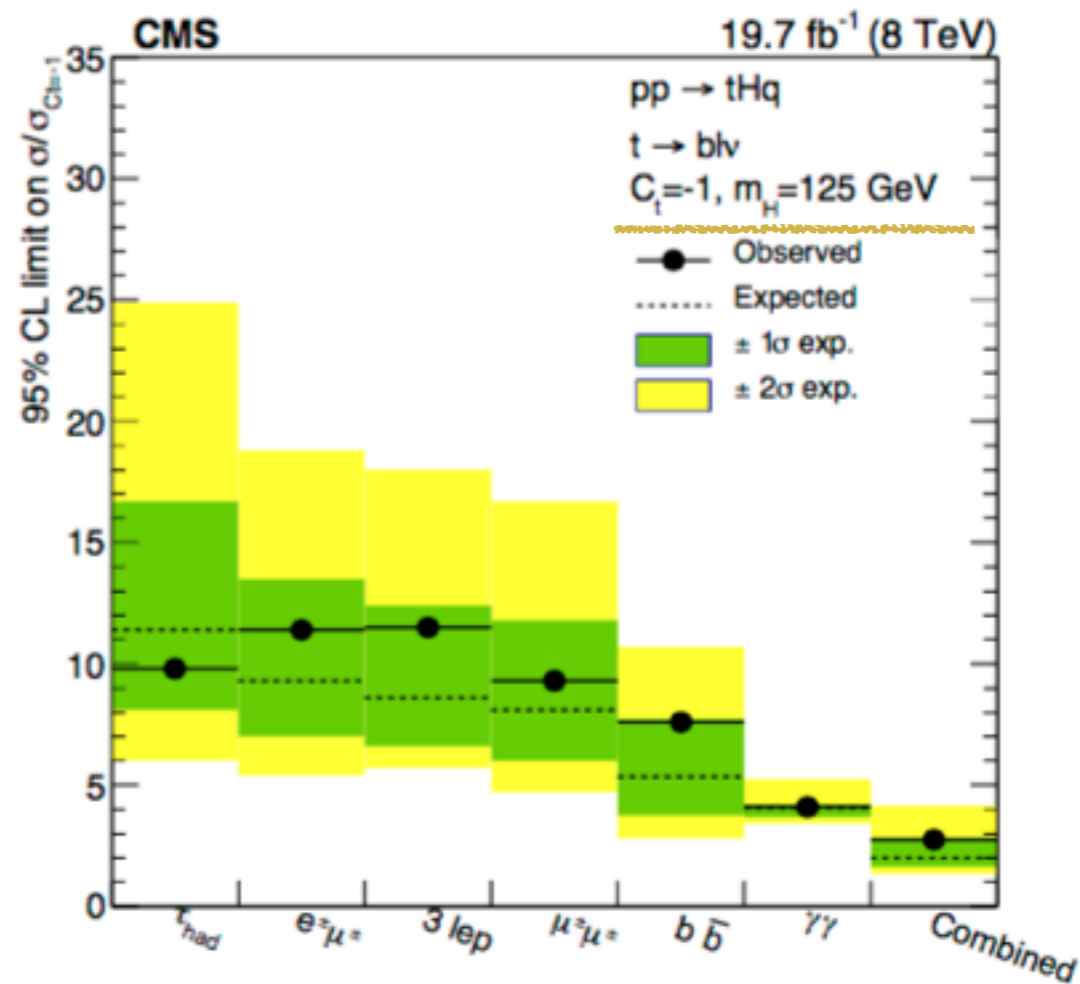
Figure 1: Dominant Feynman diagrams for the production of tHq events: the Higgs boson is typically radiated from the heavier particles of the diagram, i.e. the W boson (left) or the top quark (right).

arXiv:1509.08159

JHEP 1606 (2016) 177

Highlight some experimental results for the Higgs boson at the LHC

- CMS search for the Associated Higgs production with a Single Top Quark



Formalism from Higgs Precision (Higgscision) analysis

- Assuming that the Higgs boson h is a generic CP-mixed state, we can write the gauge-Higgs and Yukawa coupling as

$$\mathcal{L}_{hVV} = gm_W \left(g_{hWW} W_\mu^+ W^{-\mu} + g_{hZZ} \frac{1}{2c_W^2} Z_\mu Z^\mu \right) h,$$
$$\mathcal{L}_{hff} = - \sum_{f=t,b,c,\tau} \frac{gm_f}{2m_W} \bar{f} \left(g_{hff}^S + ig_{hff}^P \gamma_5 \right) f h.$$

We note $g_{hWW} = g_{hZZ} = g_{hff}^S = 1$ and $g_{hff}^P = 0$ in the SM.

Formalism from Higgs Precision (Higgscision) analysis

The amplitude for the decay process $h \rightarrow \gamma\gamma$ can be written as

$$\mathcal{M}_{h\gamma\gamma} = -\frac{\alpha m_h^2}{4\pi v} \left\{ S^\gamma(m_h) (\epsilon_{1\perp}^* \cdot \epsilon_{2\perp}^*) - P^\gamma(m_h) \frac{2}{m_h^2} \langle \epsilon_1^* \epsilon_2^* k_1 k_2 \rangle \right\},$$

where $k_{1,2}$ are the momenta of the two photons and $\epsilon_{1,2}$ the wave vectors of the corresponding photons, $\epsilon_{1\perp}^\mu = \epsilon_1^\mu - 2k_1^\mu(k_2 \cdot \epsilon_1)/m_h^2$, $\epsilon_{2\perp}^\mu = \epsilon_2^\mu - 2k_2^\mu(k_1 \cdot \epsilon_2)/m_h^2$ and $\langle \epsilon_1 \epsilon_2 k_1 k_2 \rangle \equiv \epsilon_{\mu\nu\rho\sigma} \epsilon_1^\mu \epsilon_2^\nu k_1^\rho k_2^\sigma$. Retaining only the dominant loop contributions from the third-generation fermions and W^\pm , and including some additional loop contributions from new particles, the scalar and pseudoscalar form factors are given by

$$\begin{aligned} S^\gamma(m_h) &= 2 \sum_{f=b,t,\tau} N_C Q_f^2 g_{hff}^S F_{sf}(\tau_f) - g_{hWW} F_1(\tau_W) + \Delta S^\gamma, \\ P^\gamma(m_h) &= 2 \sum_{f=b,t,\tau} N_C Q_f^2 g_{hff}^P F_{pf}(\tau_f) + \Delta P^\gamma, \end{aligned} \quad (4)$$

where $\tau_x = m_h^2/4m_x^2$, $N_C = 3$ for quarks and $N_C = 1$ for tau leptons, respectively.

In the SM, $P^\gamma = 0$, $g_{hff}^S = g_{hWW} = 1$ and $\Delta S^\gamma = 0$.

Formalism from Higgs Precision (Higgscision) analysis

Similarly, the amplitude for the decay process $h \rightarrow gg$ can be written as

$$\mathcal{M}_{Hgg} = -\frac{\alpha_s m_h^2 \delta^{ab}}{4\pi v} \left\{ S^g(m_h) (\epsilon_{1\perp}^* \cdot \epsilon_{2\perp}^*) - P^g(m_h) \frac{2}{m_h^2} \langle \epsilon_1^* \epsilon_2^* k_1 k_2 \rangle \right\},$$

where a and b ($a, b = 1$ to 8) are indices of the eight $SU(3)$ generators in the adjoint representation. Including some additional loop contributions from new particles, the scalar and pseudoscalar form factors are given by

$$\begin{aligned} S^g(m_h) &= \sum_{f=b,t} g_{hff}^S F_{sf}(\tau_f) + \Delta S^g, \\ P^g(m_h) &= \sum_{f=b,t} g_{hff}^P F_{pf}(\tau_f) + \Delta P^g. \end{aligned} \tag{6}$$

In the SM, $P^g = 0$, $g_{hff}^S = 1$ and $\Delta S^g = 0$.

Formalism from Higgs Precision (Higgscision) analysis

- Since we are primarily interested in **size** of the gauge-Higgs and top-Yukawa couplings and the **relative sign** between them, for bookkeeping purpose, we use the following simplified notations :

$$C_v \equiv g_{hWW} = g_{hZZ}, \quad C_t^{S,P} \equiv g_{htt}^{S,P}, \quad C_b^{S,P} \equiv g_{hbb}^{S,P}.$$

Results from Higgs Precision (Higgscision) analysis for Run-1 data

arXiv:1407.8236

Phys.Rev. D90 (2014) 095009

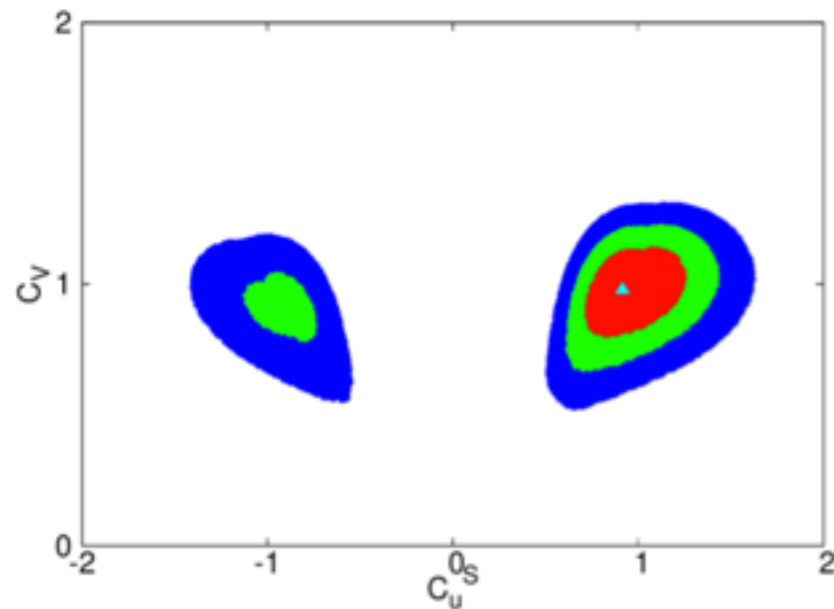


FIG. 2. The confidence-level regions in the plane of (C_u^S, C_v) of the CPC4 fit by varying $C_u^S, C_d^S, C_l^S,$ and C_v while keeping $\Delta S^\gamma = \Delta S^\beta = \Delta\Gamma_{tot} = 0$. The contour regions shown are for $\Delta\chi^2 \leq 2.3$ (red), 5.99 (green), and 11.83 (blue) above the minimum, which correspond to confidence levels of 68.3%, 95%, and 99.7%, respectively. The best-fit point is denoted by the triangle.

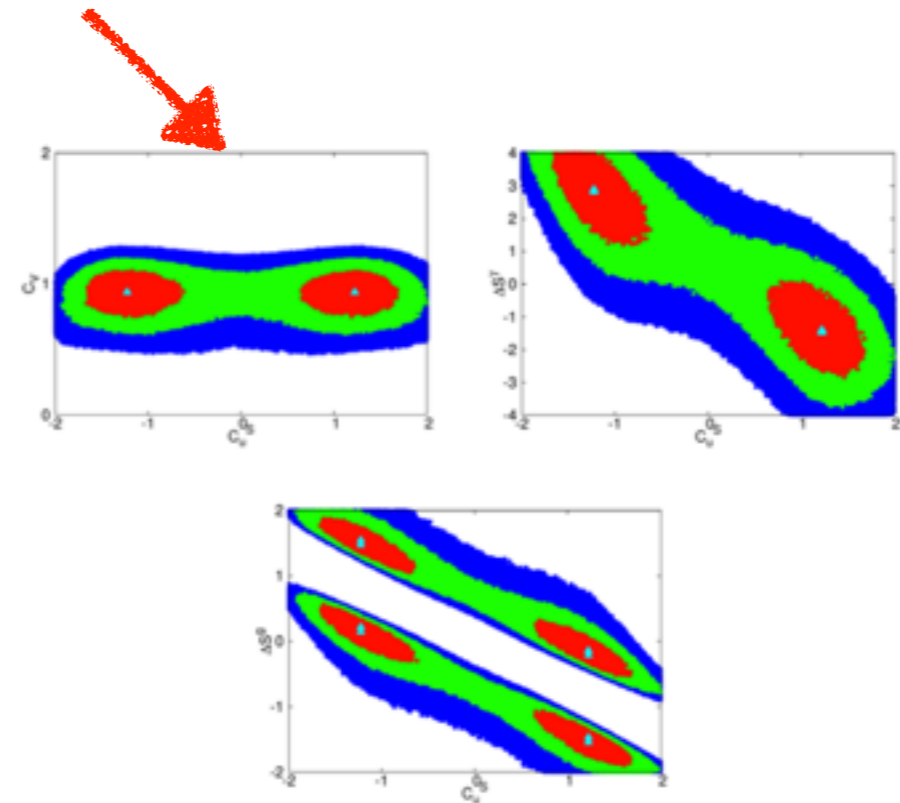


FIG. 3. The confidence-level regions in the plane of (C_u^S, C_v) , $(C_u^S, \Delta S^\gamma)$, and $(C_u^S, \Delta S^\beta)$ of the CPC6 fit by varying $C_u^S, C_d^S, C_l^S, C_v, \Delta S^\gamma,$ and ΔS^β . The contour regions shown are for $\Delta\chi^2 \leq 2.3$ (red), 5.99 (green), and 11.83 (blue) above the minimum, which correspond to confidence levels of 68.3%, 95%, and 99.7%, respectively. The best-fit points are denoted by the triangles.

Results from Higgs Precision (Higgscision) analysis for Run-1 data

As shown in Refs. [3] in which the model-independent fit to the current Higgs data is performed, the negative $C_t^S = -1$ is ruled at 95%CL if only the gauge-Higgs coupling C_v and the top-Yukawa coupling C_t^S vary. However, $C_t^S = -1$ is still allowed at 95%CL when the gauge-Higgs C_v , top-Yukawa C_t^S , bottom-Yukawa C_b^S , and tau-Yukawa C_τ^S couplings are all allowed to vary. Furthermore, if some sizable contributions to ΔS^γ and ΔS^g due to additional new particles running in the loop are assumed, a broad range of C_t^S between -2 and $+2$ is still consistent with the current Higgs data.

Results from Higgs Precision (Higgscision) analysis for Run-1 data

arXiv:1407.8236

Phys.Rev. D90 (2014) 095009

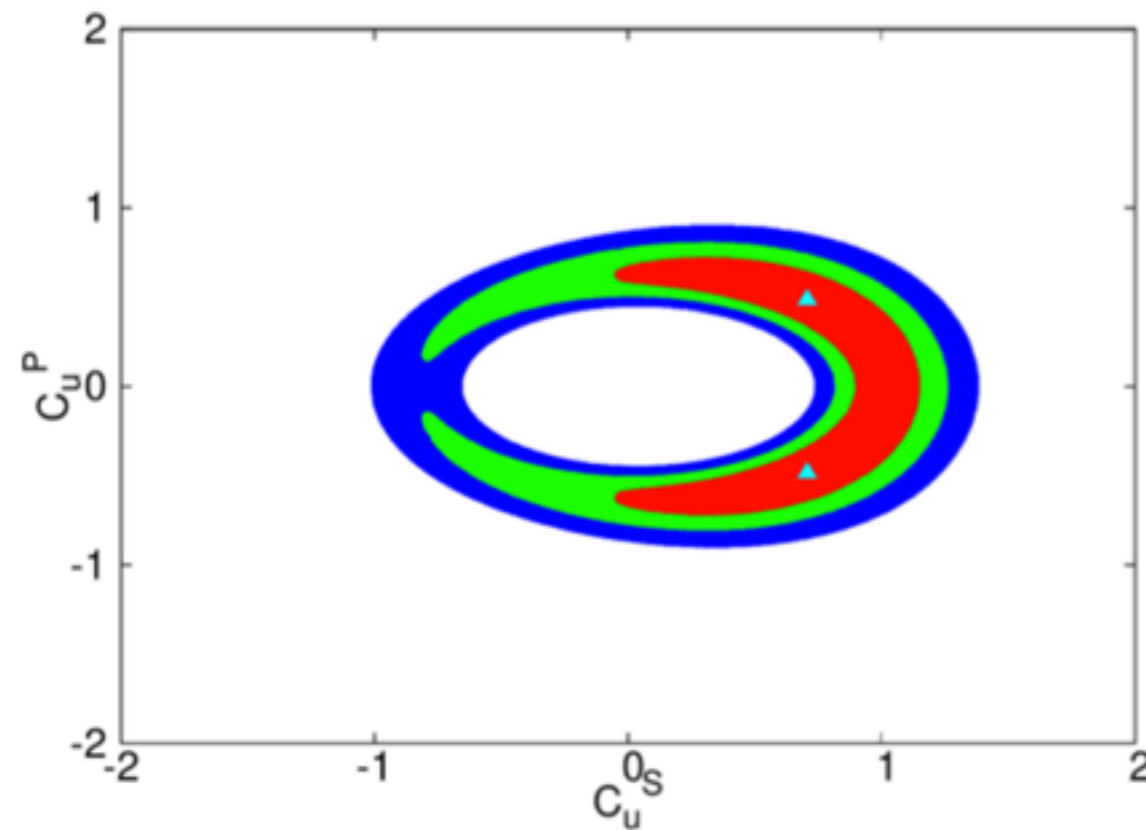


FIG. 4. The confidence-level regions of the fit by varying the scalar Yukawa couplings C_u^S and C_u^0 , and the pseudoscalar Yukawa couplings C_u^P ; while keeping others at the SM values. The description of contour regions is the same as in Fig. 2.

Probing the Top-Yukawa Coupling in Associated Higgs production with a Single Top Quark

- As well known, $t\bar{t}h$ production only depends on the **absolute value** of the top-Yukawa coupling.
- Meanwhile, in thX production, this degeneracy is lifted through the **strong interference** between the two main contributions which are proportional to the **top-Yukawa** and the **gauge-Higgs couplings**, respectively.
- Especially, when **the relative sign** of the top-Yukawa coupling with respect to the gauge-Higgs coupling is reversed, the thX cross section can be enhanced by more than one order of magnitude.

$t\bar{t}h$ production at LO

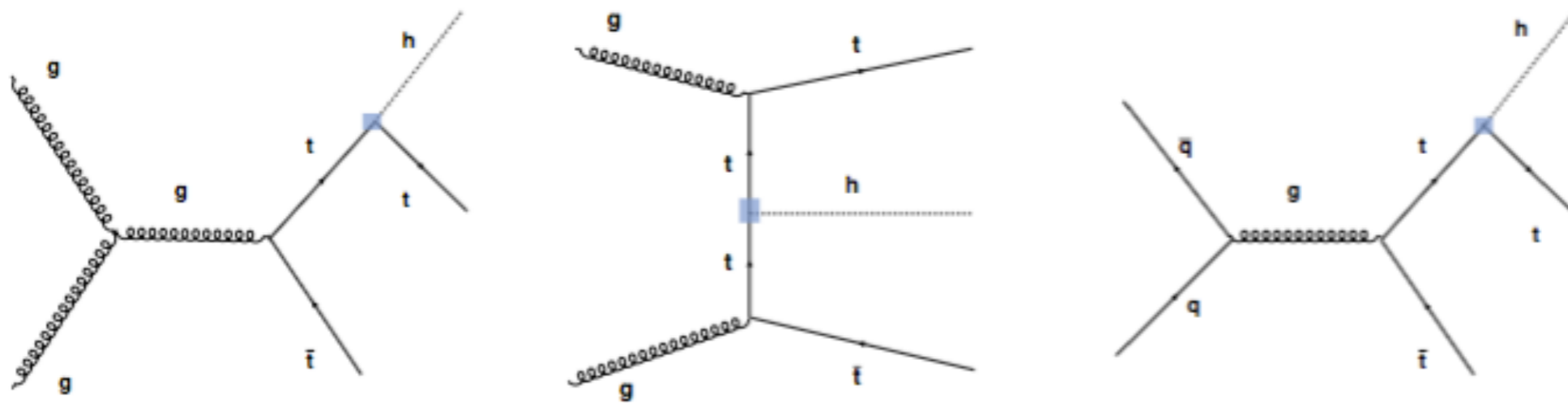


FIG. 1. Feynman diagrams contributing to $t\bar{t}h$ production at LO.

thX production with $X=j$



FIG. 2. Feynman diagrams contributing to thX production with $X = j$.

Other thX productions with $X = j\bar{b}, W, b$

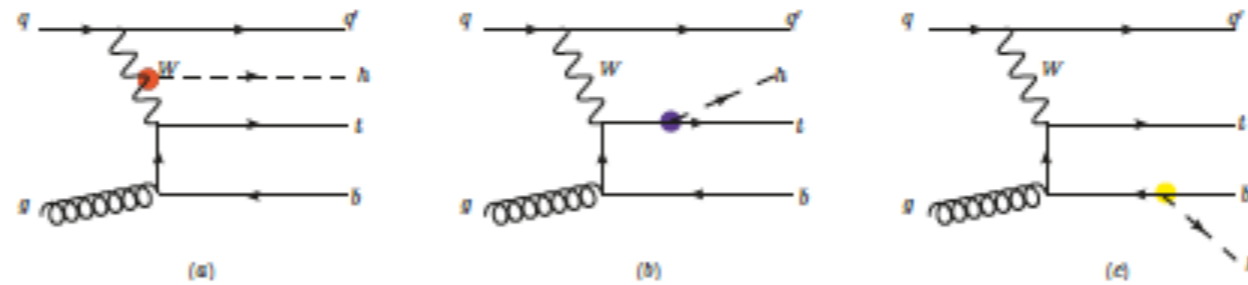


Figure 2. Some of the contributing Feynman diagrams for $qq \rightarrow thq'\bar{b}$.

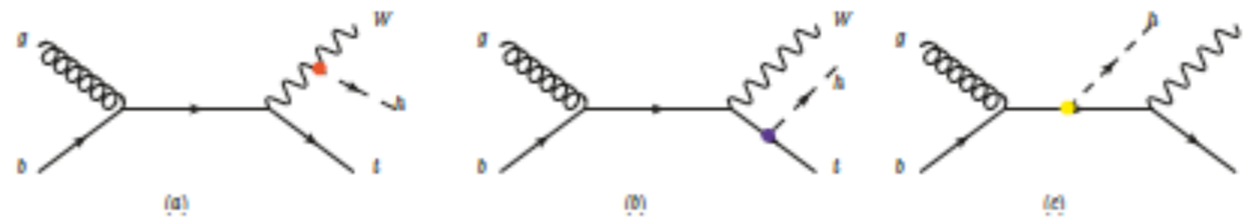


Figure 3. Some of the contributing Feynman diagrams for $gb \rightarrow thW^-$.

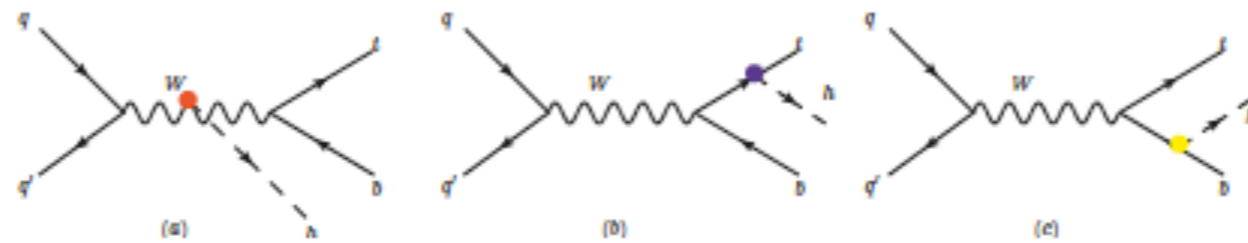


Figure 4. Contributing Feynman diagrams for $qq' \rightarrow th\bar{b}$.

Variation of cross sections for thX production

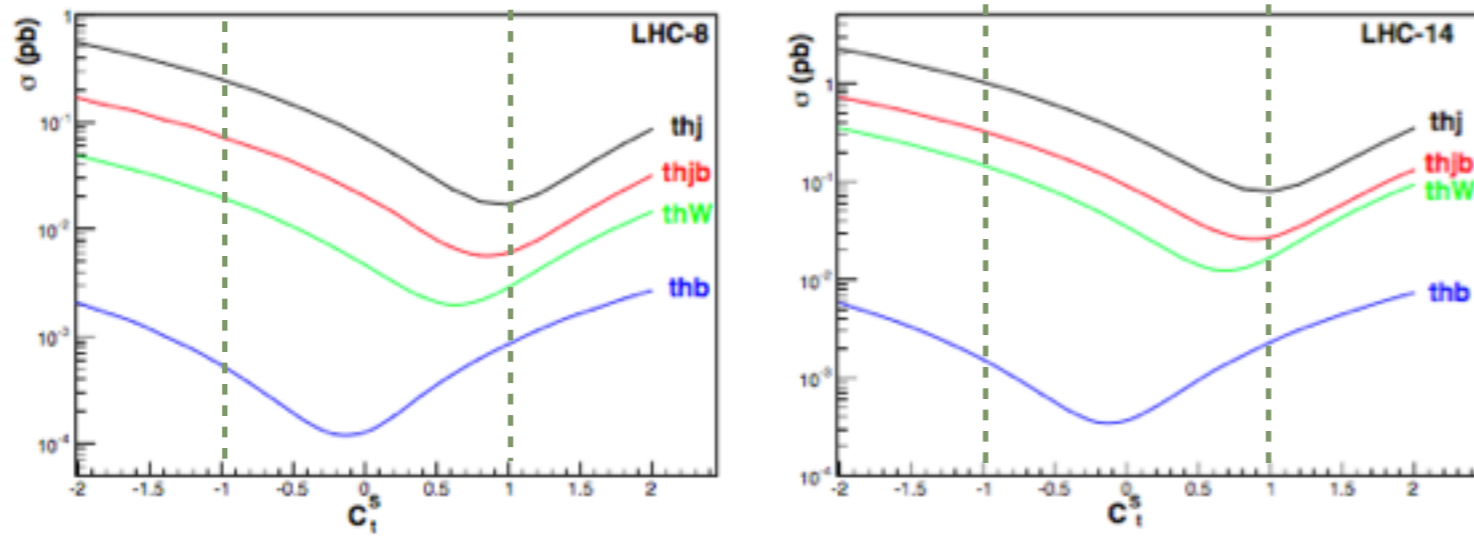


Figure 5. Variation of the total cross sections versus C_t^S for $pp \rightarrow thX$ with $X = j, jb, W, b$ in the order of the size of cross sections at (a) LHC-8 and (b) LHC-14. We have taken $C_v = C_b^S = 1$ and $C_{t,b}^P = 0$. No cuts are imposed except for the second process $pp \rightarrow thjb$ in which we applied the cuts in eq. (3.1) to remove the divergence.

	$\sigma(pp \rightarrow thX)[fb]$			
	$X = j$	$X = j + b$	$X = W$	$X = b$
$C_t^S = +1$ (SM)	79.4 (17.1)	27.1 (5.95)	17.0 (2.89)	2.32(0.833)
$C_t^S = 0$	305 (71.4)	90.0 (19.8)	34.4 (4.66)	0.368 (0.126)
$C_t^S = -1$	1030 (249)	325 (72.8)	146 (19.8)	1.52 (0.536)

Table 1. The leading-order production cross sections in fb for the processes $pp \rightarrow th + X$ at 14 TeV (8 TeV) LHC, taking $C_v = C_b^S = 1$ and $C_{t,b}^P = 0$. We have not applied any cuts except for the case with $X = j + b$ for which we required $p_{T_b} > 25$ GeV, $|\eta_b| < 2.5$; $p_{T_j} > 10$ GeV, $|\eta_j| < 5$, see text for details.

Variation of cross sections for thX production versus C_t^P

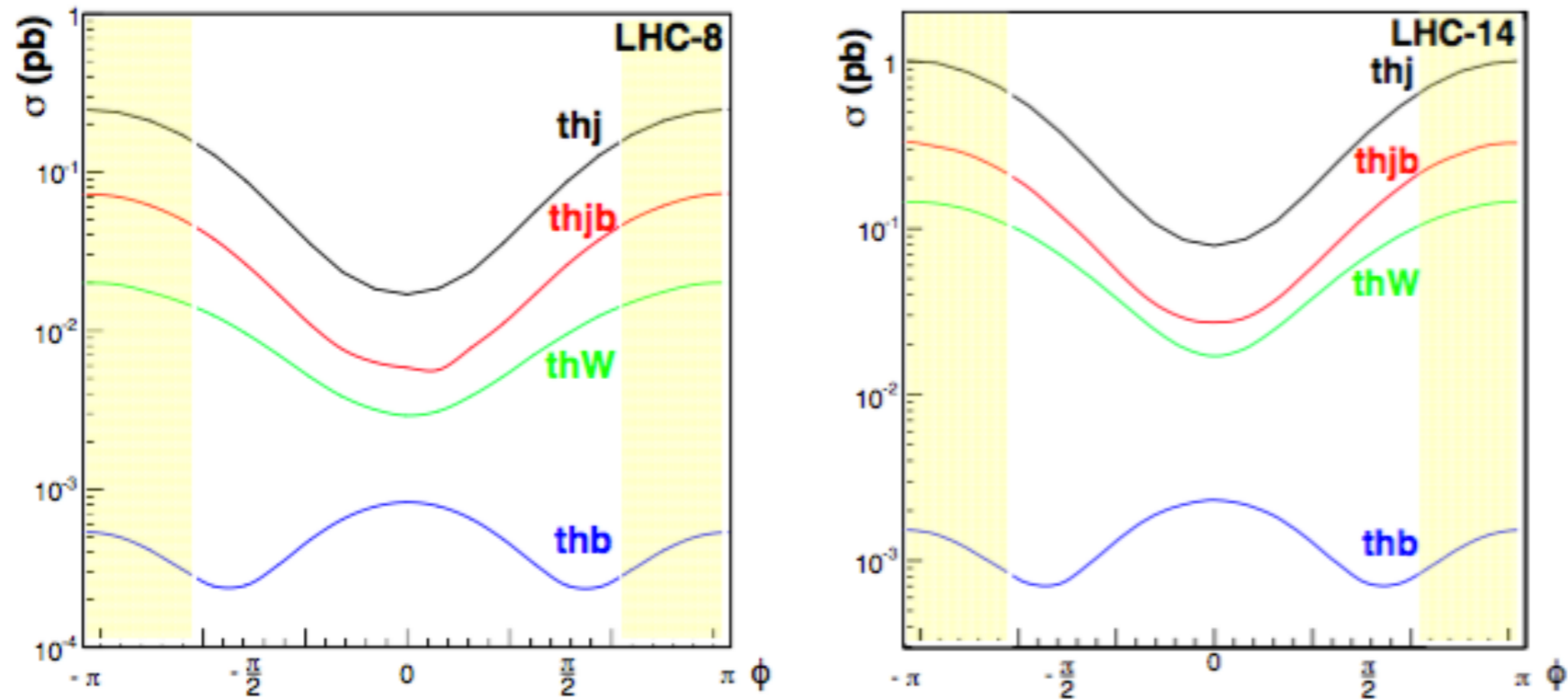


Figure 6. Production cross sections at the LHC-14 for $pp \rightarrow thj$ versus $\phi = \arctan(C_t^P/C_t^S)$ under the constraint $(C_t^S/0.86)^2 + (C_t^P/0.56)^2 = 1$. We take $C_v = 1$. The shaded regions are those disallowed at 68% C.L. by the Higgs data obtained in ref. [3].

Distinction among $C_t^S = 1, 0, -1$

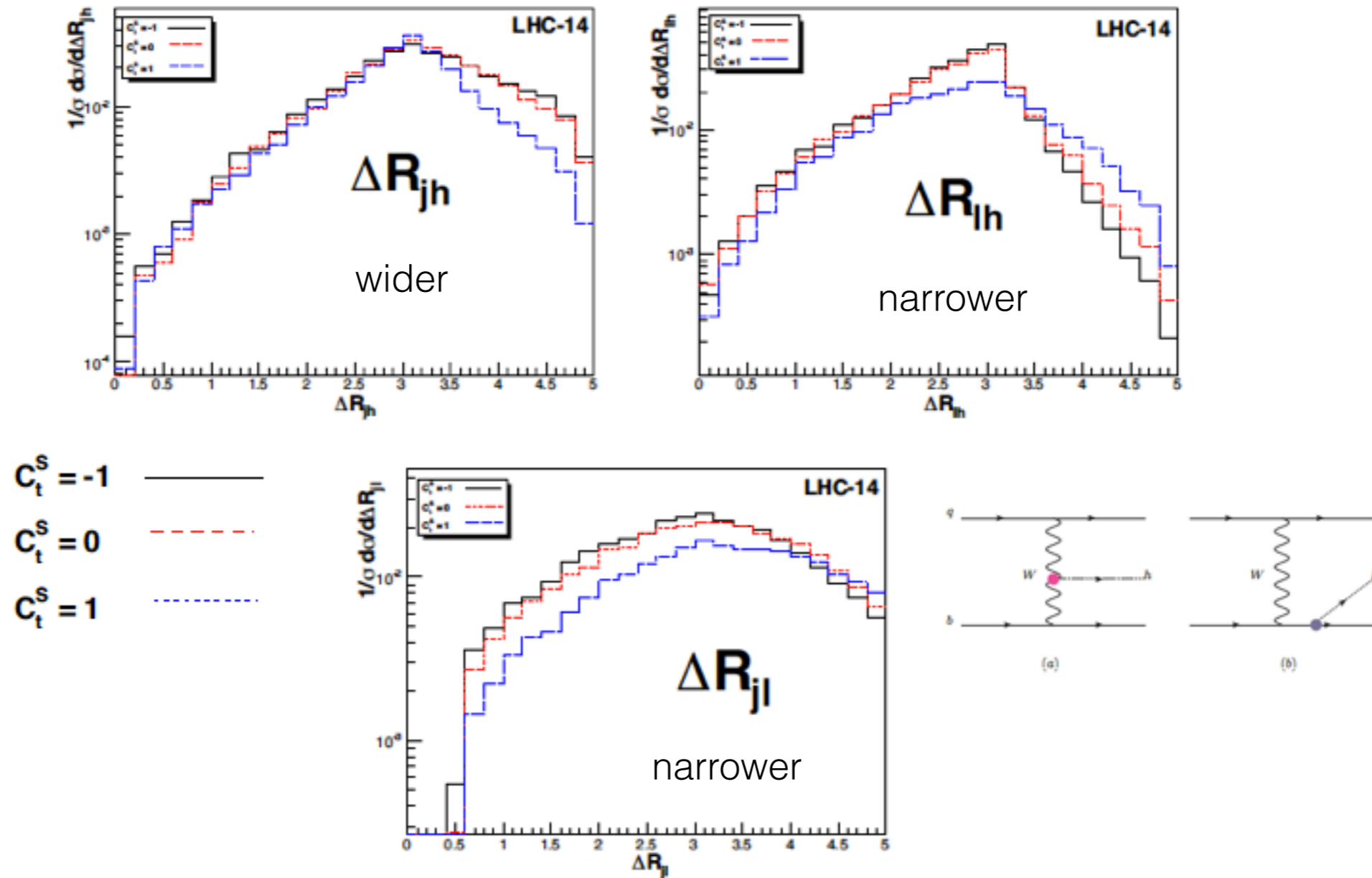


Figure 12. Normalized ΔR distributions for various pairs of particles (ℓ, j, h), where the momentum of h is reconstructed by the photon pair, for the signal process $pp \rightarrow thj$ with $C_t^S = -1, 0, 1$ followed by the semileptonic decay of the top quark and $h \rightarrow \gamma\gamma$ at the LHC-14. Behavior of b and ℓ is about the same, as they are coming from the same top quark decay. We need only one of them: ℓ .

Discussion

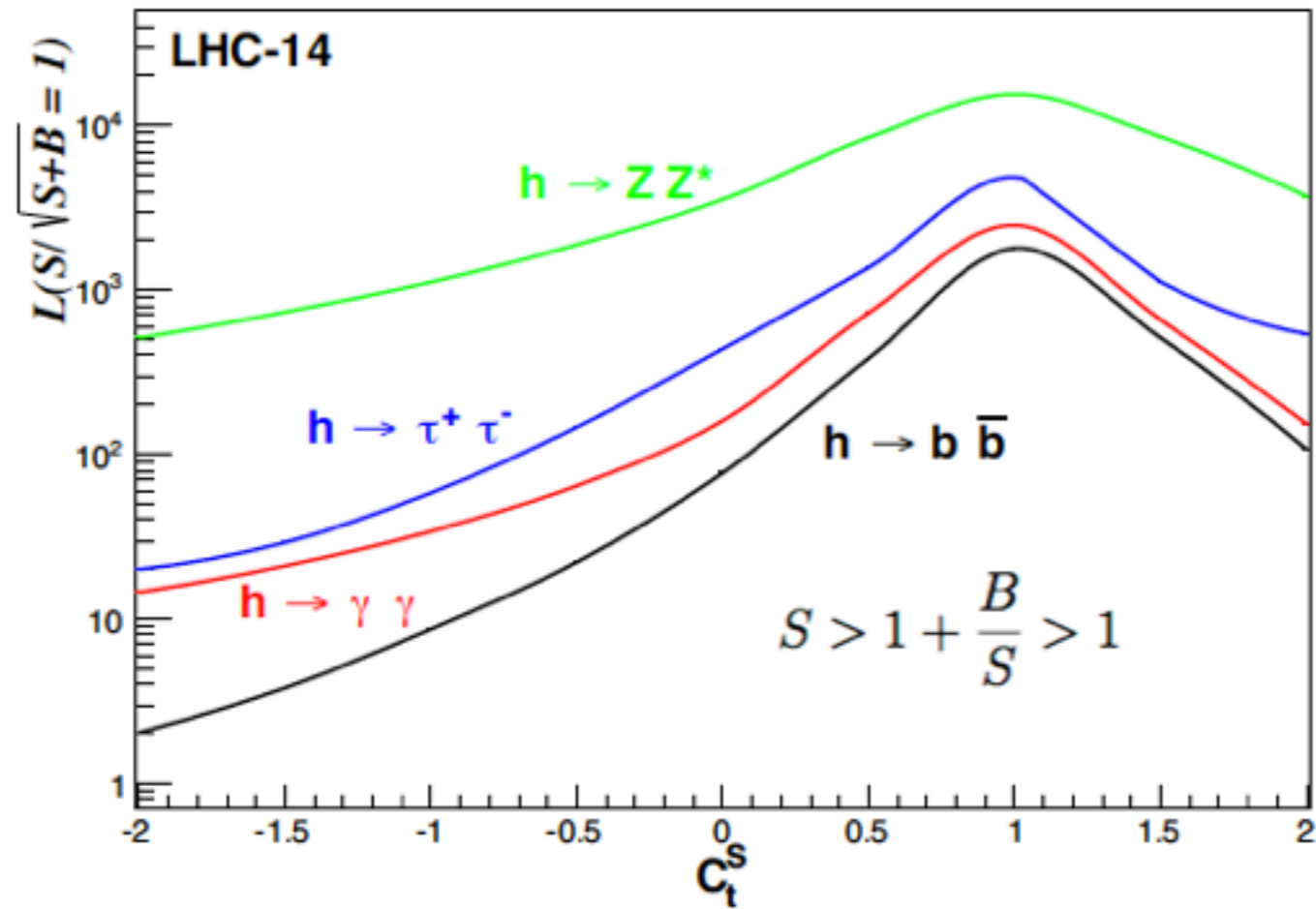


Figure 13. Required luminosities at the LHC-14 for the process $pp \rightarrow thj$ in various decay channels of the Higgs boson to achieve $S/\sqrt{S+B} = 1$. We show the channels $h \rightarrow b\bar{b}$, $\gamma\gamma$, $\tau^+\tau^-$, and $ZZ^* \rightarrow 4\ell$.

Thank You For Your Attention !!

